29th International Cosmic Ray Conference Pune (2005) **4**, 131–134

Modelling the gamma-ray emission from PSR B1259 −63

J.G. Kirk[a], Lewis Ball[b] and S. Johnston[c]
(a) Max-Planck-Institut für Kernphysik, D-69029 Heidelberg, Germany
(b) Australia Telescope National Facility, CSIRO, PO Box 276, Parkes, NSW 2870, Australia
(c) Australia Telescope National Facility, CSIRO, PO Box 76, Epping, NSW 1710, Australia
Presenter: J.G. Kirk (John.Kirk@mpi-hd.mpg.de), ger-kirk-J-abs1-og22-oral

The high-energy gamma-ray emission discovered using the H.E.S.S. telescopes from the binary system PSR B1259 −63, is modelled using an extension of the approach that successfully predicted it. We find that the simultaneous INTEGRAL and H.E.S.S. data permit both a model with dominant radiative losses, high pulsar wind Lorentz factor and modest efficiency as well as one with dominant adiabatic losses, a slower wind and higher efficiency. Additional, simultaneous, X-ray and TeV data sets are needed to lift this degeneracy.

1. Introduction

The radio pulsar PSR B1259 −63 is in a highly elliptical orbit about the luminous Be star SS2883. Pulsar winds are expected to accelerate electrons to Lorentz factors of up to 10^7, leading to up-scattering of the ultra-violet photons from the Be star into the TeV range [17, 11, 5, 9]. This can happen before or after the wind passes through its termination shock [3]. However, in the case of PSR B1259 −63, the time spent by an individual electron in the unshocked wind is short compared to the time spent in the vicinity of the Be star after passing the shock. Thus, even if the shock simply isotropises the electrons without energising them, the post-shock emission should dominate over the pre-shock emission. This conclusion holds a forteriori, if, as expected, the shock transfers some of the incoming kinetic energy into nonthermal particles.

Observations using the H.E.S.S. array of imaging Čerenkov telescopes around and after the periastron passage in early 2004 detected a strong signal in the TeV range [15, 2]. The measured spectrum is in excellent agreement in both slope and absolute normalisation with that predicted by a model in which the post-shock pulsar wind electrons have a simple, single power-law distribution [11]. Significant night-to-night fluctuations in the TeV light curve as well as an overall decrease on the timescale of months were also observed by H.E.S.S., possibly correlated with variations in the unpulsed radio emission [8]. Short timescale fluctuations, especially close to periastron, can plausibly be attributed to departures from spherical symmetry in the structure of the pulsar wind or the Be star wind; the most detailed current model ascribes the variation in the unpulsed radio emission to the latter [4, 6]. These were not taken into account in the predictions of the TeV emission [11], which included only those effects arising from the variation of the stellar separation over the orbit. A model in which the TeV emission arises from proton-proton interactions in the anisotropic wind ("disk") of the Be star [9] produces short timescale features qualitatively similar to those observed, but appears to predict a flatter TeV spectrum than that seen by H.E.S.S.

In this paper, we present preliminary results from an extended version of the model of [11]. Injection of a double power-law electron spectrum, similar to that thought to be injected into the Crab Nebula by its central pulsar [7] is included, as is the transition from radiative to adiabatic loss mechanisms as the stellar separation increases.

Table 1. The model parameters. The efficiency refers to the fraction of the spin-down luminosity injected into the source as relativistic particles (assuming a source distance of 1.5 kpc). The adiabatic loss time $t_{\rm ad}$ is given in units of the light crossing time of the periastron separation (320 sec). B is the magnetic field strength in the source at periastron

Model:	$\gamma_{\rm min}$	$\gamma_{\rm p}$	$\gamma_{\rm max}$	$\gamma_{\rm w}$	B	Efficiency	$t_{\rm ad}$
A	425	10^7	5×10^7	5.5×10^4	0.3 G	10%	15
B	425	10^6	4×10^7	2.9×10^4	0.3 G	100%	0.5

2. The model

It has recently become clear [13] that the pulsar wind that fuels the Crab Nebula injects into it relativistic electrons and positrons (and possibly ions) whose energy distribution can be approximated as a double power-law: $Q(\gamma) = (\gamma/\gamma_{\rm p})^{-q_1}$, for $\gamma_{\rm min} < \gamma < \gamma_{\rm p}$ and $Q(\gamma) = (\gamma/\gamma_{\rm p})^{-q_2}$ for $\gamma_{\rm p} < \gamma < \gamma_{\rm max}$. The high-energy index is determined by the slope of the X-ray spectrum of the Crab Nebula: $q_2 \approx 2.2$, in agreement with theories of first-order Fermi acceleration at relativistic shocks [12, 1]. The low energy index follows from the slope of the radio to infra-red spectrum: $q_1 \approx 1.6$. With these values, most particles are concentrated around the lower cut-off at $\gamma = \gamma_{\rm min}$, whereas most of the energy is injected in electrons of Lorentz factor $\gamma \sim \gamma_{\rm p}$. In the Crab, $\gamma_{\rm min} \approx 100$, $\gamma_{\rm p} \approx 10^6$ and $\gamma_{\rm max} \approx 10^9$. The resulting synchrotron spectrum contains two breaks, one due to cooling and one intrinsic to the injected spectrum (at 10^{13} Hz and 10^{15} Hz in the Crab), as well as upper and lower cut-offs. If this injection spectrum is produced at the termination shock front, and if the cold upstream flow is dominated by the kinetic energy flux in electron-positron pairs, then the Lorentz factor of the wind is $\gamma_{\rm w} = \int {\rm d}\gamma\, \gamma Q(\gamma) / \int {\rm d}\gamma\, Q(\gamma)$. In the following we adopt this injection model.

In PSR B1259 $-$63, relativistic electrons and positrons in the shocked pulsar wind suffer adiabatic losses as the plasma expands away from the shock front, as well as radiative losses by synchrotron radiation and inverse Compton scatterings, primarily of the ultra-violet photons from the Be star. The energy dependence of these loss processes is different and influences the resulting distribution function. Two sets of models were constructed in [11]: one for dominant adiabatic and one for dominant radiative losses. Both were calibrated using the observed X-ray synchrotron emission, and provided accurate predictions of the TeV spectrum subsequently detected just before periastron. However, the two models imply quite different injection spectra.

As the pulsar moves away from the Be star, both the target radiation field and the magnetic field where the winds interact decrease, along with the gas pressure. For the toroidal field structure expected in a pulsar wind, the ratio of the energy densities of magnetic field and target radiation remain constant, so that, in the absence of Klein-Nishina effects, the ratio of synchrotron to inverse Compton radiation should not vary with binary phase. However, if the expansion time scales linearly with the stellar separation, adiabatic losses become more important with respect to radiative losses as the stars move apart. In the models used here, we account for this by switching between a radiative and an adiabatic loss term in the kinetic equation of the electrons at the Lorentz factor where the loss rates coincide. The losses themselves are specified by the magnetic field strength in the emission region, and t he adiabatic loss time scale at periastron.

The emitted radiation is a combination of synchrotron radiation in a uniform magnetic field and inverse Compton scattering of ultra-violet photons from the Be star. On its way from the pulsar system to the observer the inverse-Compton emission is partially reabsorbed via pair production on the stellar photons [11]. These processes are well-understood. To expedite the computations, [11] used delta-function approximations to the emissivities of both emission mechanisms. In addition to the standard assumption (of synchrotron theory) that the direction of the emitted photons is approximately that of the incoming electron, these approximations replace the energy spread of photons emitted by a given electron by an appropriate monochromatic term. On physical grounds, this approximation can be expected to give better results as the electron Lorentz factor in-

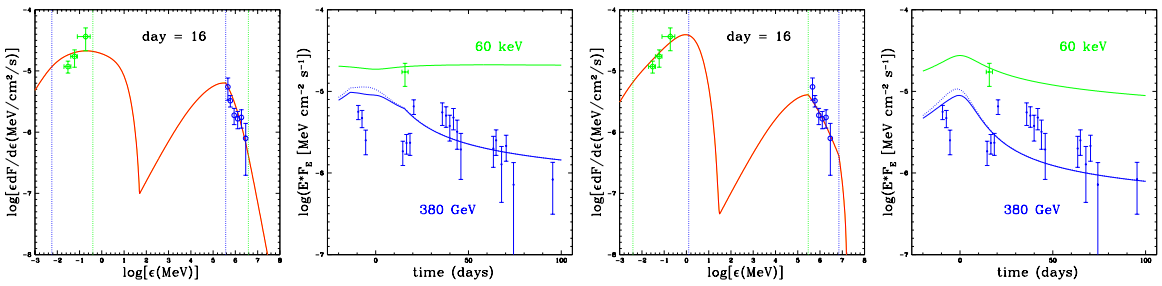

Figure 1. Spectra and light curves of models A (left) and B (right). At periastron, radiative (adiabatic) losses dominate in model A (B). The change in character of the 380 GeV light curve in Model A 17 days after periastron arises because at this epoch the corresponding electrons pass into the adiabatic loss-dominated regime.

creases and to be especially accurate in the Klein-Nishina regime of inverse Compton scattering. We have checked these approximations using a computationally more costly evaluation of the full Klein-Nishina rates and find they indeed give very accurate results, in conflict with the comparison presented in [10]. On the other hand, care must be taken with these approximations for synchrotron radiation, especially when sharp gradients in the distribution function are present. This is because the synchrotron process is equivalent to a scattering deep inside the Thomson regime, leading to a relatively broad emission cone. In this paper we use the full synchrotron emissivity, but keep the delta function approximation for inverse Compton scattering used in [11].

3. Results

Modelling the spectrum and light curve of the high energy emission during the 2004 periastron passage is made difficult by the scarcity of simultaneous TeV and X-ray data sets. The only ones available are the X-ray/soft gamma-ray spectrum detected by INTEGRAL between 14 and 17 days after periastron passage [16] and the March 2004 observations by H.E.S.S. [2]. These data are not sufficient to determine the dominant loss mechanism. To illustrate this, we consider two models, with parameters given in Table 1, where we also quote the efficiency of each model, defined as the ratio of the power injected into the emission region in the form of relativistic electrons to the pulsar spin-down power.

The TeV gamma-ray spectrum implies that the differential number of radiating electrons is roughly $\mathrm{d}\log N/\mathrm{d}\log\gamma \approx -2.5$. This can be modelled either as the result of radiative cooling of the hard injection spectrum at $\gamma < \gamma_\mathrm{p}$, or of the accumulation without energy loss of electrons injected at $\gamma > \gamma_\mathrm{p}$. The first case applies if radiative losses dominate. The second, if the losses are adiabatic.

Spectra and light-curves for Model A (radiative-loss dominated; left panels) and Model B (adiabatic-loss dominated; right panels) together with observations by INTEGRAL (green) [16] and H.E.S.S. (blue) [2] are shown in Fig. 1. The vertical blue lines depict the photon energies associated with electron Lorentz factors at which the adiabatic and radiative cooling rates are equal. At these points, a "cooling break" appears in the spectrum. The vertical green lines mark the break intrinsic to the injection function, at $\gamma = \gamma_\mathrm{p}$. The dotted curve indicates the intrinsic emission, before propagation through the radiation field of the Be star.

It is evident that Model A, cannot produce as good a fit to the (hard) X-ray spectrum as Model B, in which adiabatic losses dominate. The reason is that, in the hard X-ray range, cooling by synchrotron emission is more important than cooling by inverse Compton emission. In this case, the hardest possible model spectrum produced by cooled electrons has a photon index of -1.5. This limitation does not apply to the adiabatic-loss

dominated models. However, the data are not sufficient to reject Model A, because of the relatively large error associated with the spectrum reported by INTEGRAL ($-1.3 \pm .5$). It should be noted that in *soft* X-rays, radiative-loss dominated models produce a harder spectrum. This interesting effect, (remarked upon by many authors including [11]) arises from the transition between inverse Compton cooling at low frequencies and synchrotron cooling at higher frequencies as the scattering regime moves from Thomson into Klein-Nishina.

The key property of the models — that the TeV spectrum is formed by electrons of $\gamma < \gamma_{\rm p}$ in Model A (radiation losses) and $\gamma > \gamma_{\rm p}$ in Model B (adiabatic losses) — implies a faster pulsar wind in Model B, but also a very high efficiency. Since the computed efficiency depends on the poorly known distance to this object, values in excess of 100% are not forbidden. Nevertheless, they are uncomfortable, since the spin-down power must also provide for the kinetic energy of the bulk post-shock flow and the Poynting flux, as well as, perhaps, relativistic ions. In Model B, this problem is exacerbated by the extremely short (160 secs) adiabatic loss time, which implies a high post-shock bulk speed.

References

[1] Achterberg, A., Gallant, Y. A., Kirk, J. G., & Guthmann, A. W. 2001, MNRAS, 328, 393
[2] Aharonian, F., et al., 2005, A&A in press (astro-ph/0506280)
[3] Ball, L., & Kirk, J. G., 2000, Astroparticle Physics, 12, 335
[4] Ball, L., Melatos, A., Johnston, S., & Skjæ raasen, O. 1999, ApJ, 514, L39
[5] Chernyakova, M., & Illarionov, A. 2000, Astrophys. Space Sci., 274, 177
[6] Connors, T. W., Johnston, S., Manchester, R. N., & McConnell, D. 2002, MNRAS, 336, 1201
[7] Gallant, Y. A., van der Swaluw, E., Kirk, J. G., & Achterberg, A. 2002, in ASP Conf. Ser. 271: Neutron Stars in Supernova Remnants, 99
[8] Johnston, S., Ball, L., Wang, N., & Manchester, R. N. 2005, MNRAS, 358, 1069
[9] Kawachi, A., et al, CANGAROO Collaboration 2004, ApJ, 607, 949
[10] Khangulyan, D., & Aharonian, F. 2005, in AIP Conf. Proc. 745: High Energy Gamma-Ray Astronomy, 359–364 (astro-ph/0503499)
[11] Kirk, J. G., Ball, L., & Skjaeraasen, O. 1999, Astroparticle Physics, 10, 31
[12] Kirk, J. G., Guthmann, A. W., Gallant, Y. A., & Achterberg, A. 2000, ApJ, 542, 235
[13] Lyubarsky, Y. E. 2003, MNRAS, 345, 153
[14] Manolakou, K., & Kirk, J. G. 2002, A&A, 391, 127
[15] Schlenker, S., Beilicke, M., Khelifi, B., Masterson, C., de Naurois, M., Rolland, L., & Hess Collaboration. 2005, in AIP Conf. Proc. 745: High Energy Gamma-Ray Astronomy, 341–346
[16] Shaw, S. E., Chernyakova, M., Rodriguez, J., Walter, R., Kretschmar, P., & Mereghetti, S. 2004, A&A, 426, L33
[17] Tavani, M., & Arons, J. 1997, ApJ, 477, 439